Modal noise mitigation in a photonic lantern fed near-IR spectrograph

Fraser A. Pike,[a,*] Aurélien Benoît,[a] David G. MacLachlan,[a] Robert J. Harris,[b] Itandehui Gris-Sánchez,[c,d] David Lee,[e] Tim A. Birks,[c] and Robert R. Thomson[a]

[a]SUPA, Institute of Photonics and Quantum Sciences, Heriot-Watt University, Edinburgh, EH14 4AS, UK,
[b]Zentrum für Astronomie der Universität Heidelberg, Landessternwarte, Königstuhl 12, D-69117 Heidelberg, Germany,
[c]Department of Physics, University of Bath, Bath BA2 7AY, UK,
[d]currently at ITEAM Research Institute, Universitat Politècnica de València, 46022, Valencia, Spain
[e]STFC UK Astronomy Technology Centre, Royal Observatory, Blackford Hill, Edinburgh EH9 3HJ, UK

ABSTRACT

Recently, we have demonstrated the potential of a hybrid astrophotonic device, consisting of a multi-core fiber photonic lantern and a 3D waveguide reformatting component, to efficiently reformat the multimode point spread function of a telescope to a diffracted limited pseudo-slit. Here, we report on an investigation into the potential of this device to mitigate modal noise - one of the main hurdles of multi-mode fiber-fed spectrographs. The modal noise performance of the photonic reformatter and other fiber feeds was assessed using a bench-top spectrograph based on an echelle grating. In a first method of modal noise quantification, we used broadband light as the input, and assessed the modal noise performance based on the variations in the normalized spectrum as the input coupling to the fiber feed is varied. In a second method, we passed the broadband light through an etalon to generate a source with spectrally narrow peaks. We then used the spectral stability of these peaks as the input coupling to the fiber feed was varied as a proxy for the modal noise. Using both of these approaches we found that the photonic reformatter could significantly reduce modal noise compared to the multi-mode fiber feed, demonstrating the potential of photonic reformatters to mitigate modal noise for applications such as near-IR radial velocity measurements of M-dwarf stars.

Keywords: photonic lanterns, ultrafast laser inscription, astrophotonics, radial velocity, spectrographs, modal noise, waveguides, exoplanet detection

1. INTRODUCTION

Since the discovery of the first exoplanet, 51 Pegasi b in 1995 by the radial velocity method [1], astronomical techniques have developed and rapidly increased the number of confirmed exoplanets. The two current most productive techniques to detect exoplanets are the radial velocity method and the transit photometry method [2]. The later of these was exploited by the *Kepler Space Telescope* and involves monitoring the measured light from a star as an orbiting planet passes between the star and the telescope. Thus far, this method has identified half of the current exoplanet candidates. Another interesting and unexpected discovery from Kepler is the high potential of M-dwarf stars to host habitable near-Earth size exoplanets [3]. These specific stars have a high occurrence in the galaxy and planets around them occur twice with twice the frequency as those around a Sun-like star. Recently, impressive detections were achieved around an M-dwarf star showing planets in the habitable zone in the TRAPPIST system [4] and, in the Proxima Centauri system, the star closest to Earth [5].

One of the most productive radial velocity spectrographs is HARPS, High Accuracy Radial velocity Planet Searcher [6]. HARPS operates in the visible regime with a spectral resolving power of ~115,000, and utilises a multi-mode (MM) fiber to transport the telescope point-spread function (PSF) to the spectrograph. One of the main advantages of fiber-fed spectrographs is that the fiber enables complete mechanical de-coupling of the telescope from the spectrograph – the fiber efficiently and flexibly transports the light from the telescope to an environmentally controlled room (temperature ±0.01 K). Following the success of HARPS, several integrated fiber-fed spectrographs have been developed for different spectral ranges such as the Near Infra-Red Planet Searcher NIRPS [7].

Despite these impressive achievements, one of the main hurdles of fiber-fed spectrographs is modal noise [8-9]. By definition, a single-mode (SM) fiber fed spectrograph does not exhibit modal noise, but there are challenges in efficiently coupling seeing-limited starlight to SM fibers. To overcome these issues, Extreme Adaptive Optics (EAO) systems can be exploited but they are also extremely expensive. Counterintuitively, modal noise is not a significant issue for spectrographs fed with highly multi-mode fibers, such as is the case for HARPS. This is because the modal noise can easily be averaged out with fiber scramblers [10]. Modal noise is, in fact, most severe in spectrographs fed with fibers guiding between a few, and a few 10's of modes. Since the number of modes in the telescope PSF is inversely proportional to the wavelength, this that modal noise is most challenging in high resolution, long wavelength, near infrared spectrographs for applications such as radial velocity measurements of M-dwarfs.

With these points in mind, an ideal spectrograph for ground based applications would use a multi-mode fiber feed to efficiently capture the seeing-limited PSF, but would also utilize some additional technology that is capable of delivering the light into the spectrograph in a highly stable, and ideally diffraction-limited manner. One technology that has the potential to enable this seemingly impossible combination is a photonic device called a photonic lantern (PL) [11]. The PL is an "optically slow" waveguide transition that allows the adiabatic coupling of light between a multi-mode waveguide (e.g. a multi-mode fiber) and a set of single modes. If these single modes are suitably arranged at the input to a spectrograph, then it is logical that such a spectrograph would combine the efficiency of a multimode fiber fed system with the spectral resolution of a diffraction-limited system [12]. Recently, we demonstrated how a photonic reformatting system, which we called a hybrid reformatter (HR), based on a three-dimensional waveguide reformatting chip fabricated via ultrafast laser inscription (ULI) and a multi-core fiber (MCF) type PL, can be used to efficiently reformat the PSF of the CANARY AO system of the William Herschel telescope [13]. Here, we discuss the potential of these photonic reformatting systems to also strongly mitigate modal noise in future high resolution near-infrared spectrographs.

2. EXPERIMENTAL SETUP

To investigate the modal noise performance of various fiber feeds we constructed the bench-top spectrograph shown schematically in Fig. 1(a). This allowed us to compare the relative modal noise performance of an SM fiber feed, the HR and a commercial 50 µm MM fiber which supported 124 modes at ~1550 nm, similar to the 92 modes guided and reformatted by the HR. Fig. 1(b) presents a photograph of the photonic reformatter, with (b-1) the ULI fabricated waveguide reformatter, (b-2) the MCF and (b-3) the PL transition. A SM fiber-coupled broad-band amplified spontaneous emission (ASE) source (Thorlabs FL7002-C4) centered on 1560 nm with a bandwidth of approximately 75 nm was used for all the characterization. An additional bandpass filter with a full width at half-maximum (FWHM) transmission band of 12 nm is inserted into the beam path to avoid the requirement for cross-dispersion at the output. An echelle grating (EG) with 63° blaze angle and 31.6 lines·mm^{-1} is used to generate high spectral dispersion and a 2 inch square silver mirror (M1) is used to fold the spectrograph and achieve a more compact footprint. The dispersed images are recorded using a Hamamatsu InGaAs camera that is composed of 256 × 320 pixels with a square pixel size of 30 µm. The magnification of the spectrograph is ~20. Facet images of the various devices, together with near-field images of the light emitted from the facet are presented in Figs. 1(c-h): SM in Fig. 1(c-d), MM in Fig. 1(e-f) and the HR in Fig. 1(g-h). The bench top spectrograph has a resolving power of ~9,500, ~7,000 and ~3,500 when fed with light via the SM, HR, and MM fiber feeds respectively.

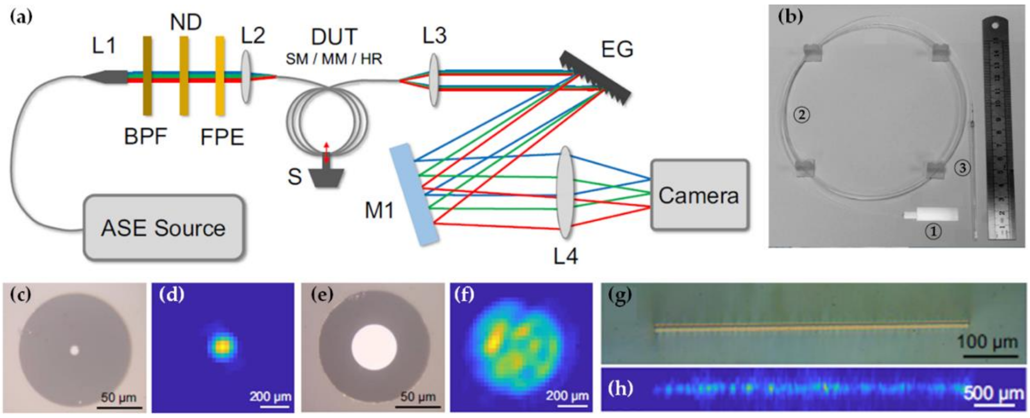

Figure 1. (a) Schematic of the bench-top spectrograph with the ASE source passing through the bandpass filter (BPF), the neutral density (ND) and the Fabry-Perot Etalon (FPE). The light is then coupled into the device under test (DUT) which is used to feed the spectrograph. A speaker "S" could be used to agitate the DUT for additional scrambling. The dispersion of the spectrograph is generated by the echelle grating (EG) and the spectrum is recorded by the InGaAs camera after reflection on the 2 inch silver mirror M1. (b) Picture of the full HR with the pseudo-slit reformatter in (1), the multicore fiber in (2) and the photonic lantern transition in (3). Pictures of the cross section and near field intensity output for the SM (c-d), the MM (e-f) and the HR (g-h).

The aim of our study was to investigate and compare the modal noise performance of the various fiber feeds. To do so, we used two approaches. In the first, we used broadband light as the input, and assessed the modal noise performance by statistically quantifying the variations in the normalized spectrum we acquired as the input coupling to the fiber feed was varied. In the second method, we passed the broadband light through an etalon to generate a source with spectrally narrow peaks. We then used the measured stability of these peaks as the input coupling to the fiber feed was varied and used this stability as a proxy for the modal noise.

2.1 Modal noise investigation using a broadband source

The modal noise effect manifests itself as variations in the shape of the acquired spectrum as the input coupling is varied. We therefore chose to acquire 60 different spectra for 60 different input coupling conditions. The data was then processed using two steps: (i) divide each of the 60 spectra by the average spectrum across all 60 in order to obtain 60 "absolute difference" spectra, and (ii) normalize each of the absolute difference spectra such that average normalized difference for each is 1. The values of all 60 of these normalized difference spectra were then plotted to generate a single histogram, the width of which represents the variations in the shape of the spectra across all 60 measurements. Fig. 2 presents the main results of this study with an example of raw images acquired for the SM feed (Fig. 2(a)), the multi-mode fiber feed with speaker shaking (MMS) (Fig. 2(b)), the HR feed (Fig. 2(c)) and the HR feed with speaker shaking (HRS) (Fig. 2(d)). Fig. 2(e) presents the histograms of the normalized difference spectra for DUT. The standard deviation of the Gaussian fit to the data in Fig. 2(e) is also shown for each DUT and indicates a factor of ~2 reduction between the MMS and the HR, and a factor of 5.7 between the MMS and the HRS. These results demonstrate that a significant modal noise mitigation by using the HR in comparison with the MM with a similar number of guided modes, and that this mitigation can be further enhanced by mechanical agitation.

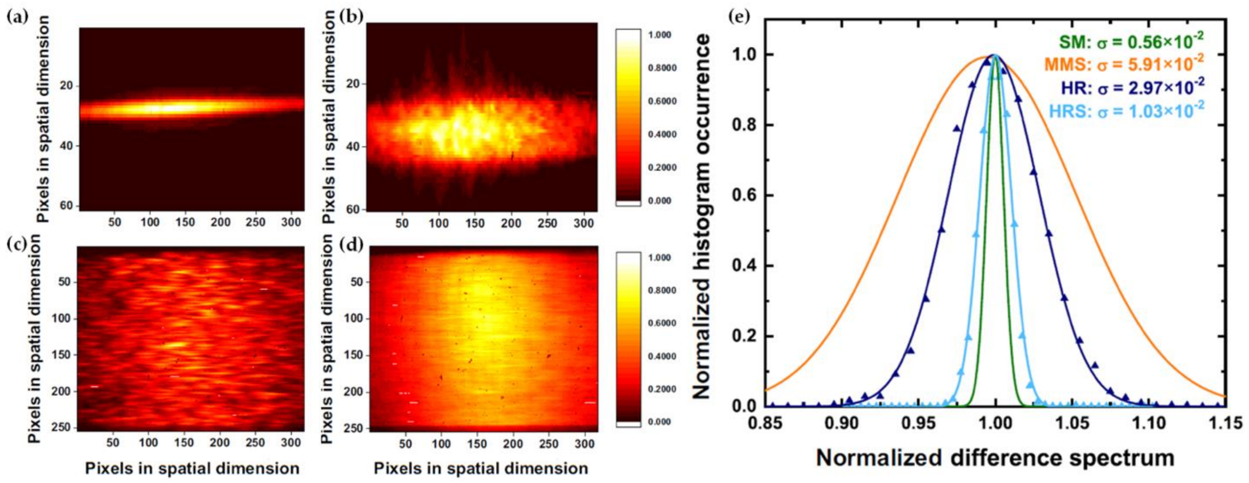

Figure 2. Normalized intensity map recorded using a broadband spectrum with the InGaAs camera for (a) the SM, (b) the MMS, (c) the HR, and (d) the HRS fiber feeds. (e) Histograms of the normalized difference spectra spectrum for the SM (green curve), the MMS (orange curve), HR (dark blue triangles), and HRS (light blue triangles) DUTs. Inset: standard deviation value for the DUT.

2.2 Modal noise investigation discrete spectral peaks

The previous study provides us with a first insight into how the modal noise impacts the acquired spectra, but it does not deliver an intuitive quantification of how modal noise would impact future astronomical measurements. To address this, we inserted a Fabry-Pérot etalon into the input beam path to convert the light source from a smoothly varying broadband source into several discrete peaks. We then investigated how the barycenters of these peaks are affected by modal noise. To match our requirements, the spectral peaks must be sufficiently spaced to resolve them on the detector array. To do that, we chose an off-the-shelf Light Machinery etalon which had a free spectral range of ~1 nm at 1550 nm and generated peaks with a full width half maximum spectral width of 40 pm. It is important to note that when examining the modal noise with such narrow peaks, we are effectively observing the modal noise that would be present in a spectrograph with a resolving power of ~40,000, even though the resolving power of the spectrograph is only ~9,500 when fed with light via the SM fiber, ~7,000 when fed with light via the HR, and ~3,500 when fed with light via the MM fiber.

Fig. 3 presents examples of raw images acquired by the spectrograph InGaAs detector array when using (a) the SM feed, (b) the MMS feed, (c) the HR feed, and (d) the HRS feed. To assess the modal noise performance of each DUT, we changed the input coupling into the DUT 60 times and acquired 60 individual spectra. For each spectrum, we determined the barycenter of each peak using a Gaussian fit. These barycenters were then plotted as a histogram and a Gaussian fit was made to this histogram. For our purposes, the standard deviation of this Gaussian fit – in effect the stability of the barycenter - was used as a quantification of the modal noise. Fig. 3(e) shows a plot of the barycentre stability for each spectral peak when using either the MM (red points), MMS (orange points), SM (green squares), HR (dark blue triangles) and HRS (clear blue triangles) to feed the spectrograph. The careful reader will observe that the peaks for each DUT are not aligned with each other; this is because the output of each DUT was not placed in an identical position relative to the spectrograph. These measurements show a clear impact of using the HR over the MM fiber to feed the spectrograph, but this improvement is expected due to the physical size of the HR output. It is also clearly apparent that shaking the MCF of the HR further increases the stability of the barycenters close to level of those generated by the SM fiber feed - the measurement limit of this characterization system.

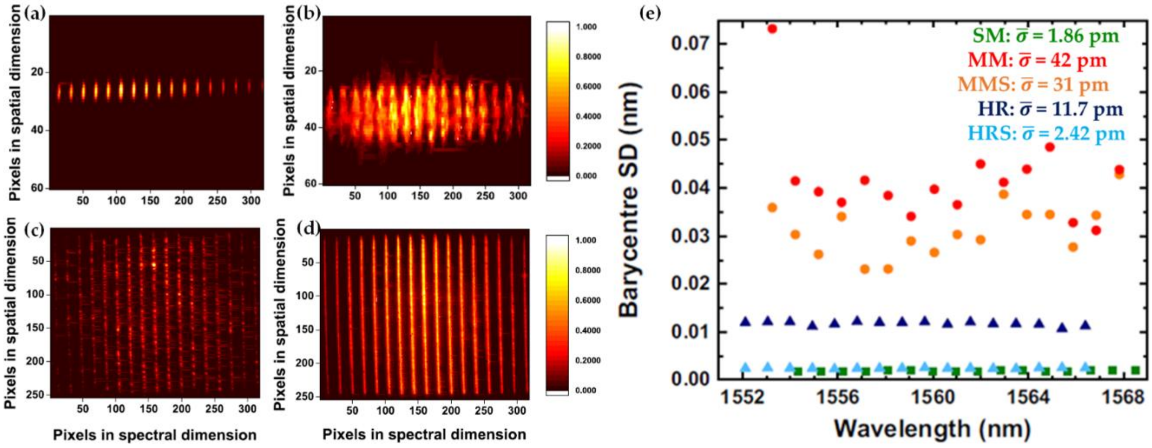

Figure 3. Raw data recorded by the InGaAs camera when passing the broadband source through a Fabry-Pérot etalon and using with the (a) SM, (b) MMS, (c) HR, and (d) HRS fiber feeds. (e) Evolution of the standard deviation of the etalon peak stability as a function of the average wavelength for the SM (green squares), the MM (red points), MMS (orange points), the HR (dark blue triangles), and the HRS (light blue triangles). Inset: Standard deviation mean values for each DUT corresponding to the average value of the barycenter precision.

2.3 Laboratory environment corrections

High precision spectrographs require an environment with high temperature stability. In contrast, our spectrograph was simply constructed in a basic laboratory without high temperature control. It is therefore important to understand and quantify how the temperature instability of the laboratory has affected our measurements. To do this, we can assume that since temperature instabilities will primarily cause refractive index changes in the ambient air and thermal drifts in the optomechanical mounts, these thermal drifts will impact the position of all of the etalon peaks in the same manner. Under this assumption, we can then use the average shift of the etalon peaks from their average position (across the 60 measurements) as a proxy for the thermal drift. As might be expected, the magnitude of this "thermal proxy" was found to vary slowly over the 60 measurements with a full range of ∼8 pm. In order to observe the effect of only the modal noise, without the influence of this thermal drift, we subtracted the relevant thermal proxy from each spectrum, and then re-evaluated the barycenter precisions which are presented in Fig. 4 for the SM and the HRS. In comparison to the results presented in Fig. 3(e), the barycenter precisions represent an improvement factor of ~6 for both DUTs. It is important to emphasize that the data obtained with the SM fiber feed merely represents the measurement limit of our system, and although the data with the HRS is now well overlapped with the data for the SM, it does not mean that the HRS has achieved the same modal noise performance of a SM fiber feed. Indeed, with an improved characterization system in the future, we would sensibly expect the two data sets to separate again, with the SM data set eventually exhibiting improved stability.

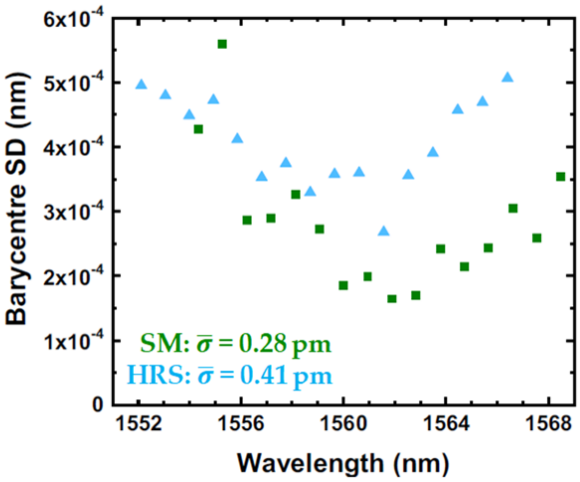

Figure 4. Barycenter stability of each etalon spectral peak as a function of the average wavelength after subtracting the relevant "thermal proxy" for each data set. Inset: Average values of the standard deviation for the SM and the HRS.

3. CONCLUSIONS

We investigated the modal noise performance of a hybrid photonic reformatting technology based on a multi-core fiber photonic lantern and a ULI fabricated 3D reformatting component that reformats the output of the multi-core fiber to a diffraction-limited pseudo-slit. A custom spectrograph was built to investigate and compare the modal noise performance of the HR with two reference devices: a SM and a MM fiber that supported a similar number of guided modes. We used two methods to quantify the strength of the modal noise. In both cases, the potential of the HR itself is highlighted as a route to improve the modal noise and resolution of the spectrograph in comparison to a MM fiber feed. By using a speaker to agitate the multi-core fiber we demonstrate that the modal noise of the HR can be improved further. After accounting for variations in the acquired spectra due to laboratory temperature shifts, we demonstrated that the HRS results in spectra that are close in stability to those measured using the SM fiber feed – although we again emphasize that the data obtained with the SM fiber feed merely represents the measurement limit of our system. We conclude that these experimental results demonstrate the potential of photonic reformatting devices that combine diffraction-limited behavior with modal noise mitigation in multi-mode operation and the relevance of this technology to provide high resolution fiber fed spectrographs. For more details on the experiments discussed here, we refer the interested reader to [14].

4. ACKNOWLEDGMENTS

This work was funded by the UK Science and Technology Facilities Council (STFC) – STFC grant no. ST/N000625/1, and by the European Union's Horizon 2020 research and innovation program under grant no. 730890 (OPTICON – Optical Infrared Coordination Network for Astronomy). FAP acknowledges support via an Engineering and Physical Sciences Research Council (EPSRC) iCASE studentship part funded by Renishaw.

5. REFERENCES

[1] Mayor, M., Queloz, D., "A Jupiter-mass companion to a solar-type star," Nature 378, 355 (1995).
[2] Borucki, W. J., Summers, A. L., "The photometric method of detecting other planetary systems," Icarus, 58(1), 121-134 (1984).
[3] Dressing, C. D., Charbonneau, D., "The occurrence rate of small planets around small stars," The Astro. Jour. 767(95) (2013).
[4] Gillon, M., Triaud, A., Demory, B. O., et al., "Seven temperate terrestrial planets around the nearby ultracool dwarf star TRAPPIST-1," Nature 542, 456-460 (2017).
[5] Anglada-Escudé, G., Amado, P. J., Barnes, J., et al., "A terrestrial planet candidate in a temperature orbit around Proxima Centauri," Nature 536, 437 (2016).

[6] Mayor, M., Pepe, F., Queloz, D., et al., “Settings new standards with HARPS,” The Messenger 114, 20-24 (2003).
[7] Blind, N., Conod, U., Wildi, F., “Few-mode fibers and AO-assisted high-resolution spectroscopy: coupling efficiency and modal noise mitigation,” Adaptive Optics for Extremely Large Telescopes 5 (AO4ELT5) (2017).
[8] Hill, K. O., Tremblay, Y., Kawasaki, B. S., “Modal noise in multimode fiber links: theory and experiment,” Opt. Lett. 5(6) (1980).
[9] Rawson, E. G., Goodman, J. W., Norton, R. E., “Analysis and measurement of the modal-noise probability distribution for a step-index optical fiber,” Opt. Lett. 5(8) (1980).
[10] Baudrand, J., Walker, G. A. H., “Modal Noise in High-Resolution, Fiber-fed Spectra: A Study and Simple Cure,” PASP 113, 851-858 (2001).
[11] Birks, T. A., Gris-Sánchez, I., Yerolatsitis, S., et al., “The photonic lantern,” Adv. In Opt. and Phot. 7, 107-167 (2015).
[12] Bland-Hawthorn, J., Lawrence, J., Robertson, G., et al., “PIMMS: photonic integrated multimode microspectrograph,” Proc. SPIE 7735, 77350N (2010).
[13] MacLachlan, D. G., Harris, R. J., Gris-Sánchez, I., et al., “Efficient photonic reformatting of celestial light for diffraction-limited spectroscopy,” MNRAS 464(4), 4950–4957 (2017).
[14] Pike, F. A., Benoit, A., MacLachlan, D. G., et al., “Modal noise mitigation for high-precision spectroscopy using a photonic reformatter,” MNRAS 497, 3713-3725 (2020).